

Cite this: DOI: 10.1039/c0xx00000x

www.rsc.org/xxxxxx

ARTICLE TYPE

Oscillating fronts produced by spinodal decomposition of metastable ordered phases

Ezequiel R. Soulé,^a Alejandro D. Rey^b

^a Institute of Materials Science, University of Mar del Plata and CONICET, J. B. Justo 4302, Mar del Plata, Buenos Aires 7600, Argentina; E-mail: ersoule@fi.mdp.edu.ar

^b Department of Chemical Engineering, McGill University, 3610 University Street, Montreal, Quebec H3A 2B2, Canada; E-mail: alejandro.rey@mcgill.ca

Received (in XXX, XXX) Xth XXXXXXXXX 20XX, Accepted Xth XXXXXXXXX 20XX

DOI: 10.1039/b000000x

Abstract. Mesophase-particle mixtures are emerging functional material systems whose structure, dynamics and formation through phase transitions is poorly understood. In this paper novel phase transitions in a system of coupled conserved and non-conserved order parameters – a mixture of liquid crystal and nanoparticles – are studied via phase-field modelling, in conditions where an intermediate phase, which is unstable to composition fluctuations, can be formed between the initial supercooled phase and the new stable phase. The paper analyzes the formation, stability and evolution of this intermediate phase and how it impacts the transformation of an isotropic phase when it is quenched with single and double temperature jumps to form a calamitic nematic phase. It is found that the intermediate phase forms through a front-splitting mechanism and grows for some time but eventually decays through a spinodal decomposition starting at the interface and propagating to the bulk, producing a moving oscillating front. It is found that this phenomenon can be triggered solely by the presence of the interface even in absence of composition fluctuations in the bulk. Spinodal decomposition initiated by thermal fluctuations also generates a moving oscillating front (because the intermediate phase was formed by a moving front). In consequence, the velocity of the moving front changes from a small value at short time (interface-induced spinodal), to a large value at some finite time (moving bulk spinodal). The effect of a double quench was also analyzed and it is found that the oscillating front can be confined to a region close to the interface (“mushy” region), and the isotropic phase (originally of infinite extension) can be confined to a region close to the oscillating front, generating a very atypical phase morphology.

1. Introduction

Phase transformations play an important role in material science and engineering^{1,2}. In the most simple case where only two phases (the supercooled phase A and the stable phase B) are involved, phase separation proceeds through the well-known mechanisms of nucleation and growth (NG) or spinodal decomposition (SD), and different material morphologies can be generated, typically droplets or co-continuous structures. Even in this relatively simple case, more complex structures or patterns can be produced by interfacial instabilities in the presence of thermal or mass diffusion, leading to cellular structures, dendritic growth, and more. Complex non-equilibrium structures can also be produced solely by the movement of the interface^{3,4}. If the existence of a third phase is possible, even if it is metastable and not observed at equilibrium, it can be formed during the process and a more complex dynamics, leading to a richer variety of structures which have been observed experimentally⁵⁻⁷ and predicted in many simulations⁸⁻¹⁶. The most simple case is when there is a metastable phase (M) intermediate between A and B phases, and the A-to-B transformation proceeds through the

sequence A→M→B. Traditionally it was considered that the higher nucleation rate of the M phase was responsible for this, but in the last decades a mechanism of “front splitting”, where a single B-A interface can spontaneously split into B-M and M-A interfaces has been proposed and widely studied. For the case where the phase structure is described by a non-conserved order parameter (NCOP), it was found that a necessary and in some cases sufficient condition for this to happen was that the M-A interface moves faster than the B-M interface^{8,9}; a typical NCOP relevant to this paper is the quadrupolar tensor order parameter that describes order and orientation in nematic liquid crystals¹⁷. The interface splitting process is schematically shown in figure 1(A) for the case where the different phases can be represented by different values of a generic NCOP, here denoted by Ψ at a given time “ t ”. An interesting conclusion is that the metastable phase grows unbounded with time. Similar analysis was performed for a conserved order parameter (COP) too¹¹, the results were similar but in this case the metastable phase can either grow unbounded or have a finite lifetime depending on the degree of undercooling; a typical COP relevant to this paper is the concentration of a

species in a binary mixture.

In previous works, a system of coupled COP and NCOP was analyzed^{12,13,14}. This last case corresponds for example to a binary mixture (where the concentration is conserved in the sense that it obeys mass conservation), with an ordered phase (the order is described by a non-conserved variable as it can be created or destroyed), and it has a more complex dynamic behavior than the cases of pure COPs (isotropic binary mixture) or NCOPs (pure nematic liquid crystal). The case where the metastable state is a local minimum with respect to the COP (metastable isotropic-isotropic phase separation) was previously analyzed in different situations; depending on the temperature-concentration location of the mixture in the equilibrium phase diagram, different front-splitting mechanisms were observed (with kinetic or thermodynamic origin), leading to different phase formation structures and different temporal dynamics. The opposite case, where the metastable state is a local minimum with respect to the NCOP (metastable homogeneous ordered phase), has also been analyzed theoretically^{15,16}. In this situation, the metastable ordered phase is formed by a front-splitting mechanism, but then this metastable phase undergoes spinodal decomposition, generating a fine structure of alternating isotropic and ordered phases. This structure emerges at the spatial location of the original interface and moves towards the bulk as a moving front. So there is a “leading” front (the interface separating undercooled isotropic and metastable ordered phase), and an “oscillating” front (which separates the homogeneous metastable phase and the region of alternating isotropic and ordered phase), where the formation of the leading front precedes the oscillating front. A two-dimensional version of this is schematically illustrated in figure 1(B) (here a planar front in two dimensions is illustrated, so within the region of spinodal decomposition order and composition can fluctuate in the two directions). Figure 1B shows in detail the sequence of material processes: (1) a thermal quench of the isotropic phase (black rectangle) results in (2) the nucleation of the ordered phase (left white patch) and formation of the front (white-black interface), subsequently (3) front splitting results with the emergence of the intermediate ordered phase (gray area) that grows (white right-pointing arrow) by the motion of a leading front (gray-black interface), and (4) the instability of the intermediate phase generates the equilibrium (co-continuous black and white areas) phases which is the oscillating moving front region (white right-pointing arrow). Previous works^{15,16} analyzed the effect of undercooling and mobility on the formation of the metastable front and the oscillating front in a generic phase-field model.

Note that the formation of the leading front is a regular front-splitting process as observed in refs [8-14] and its behavior was analyzed in those references. The key difference between the previous and the present work is that the intermediate phase is unstable and this leads to a different dynamics and structure formation. Note also that the situation analyzed in refs [11-14] can coexist with the situation considered here, that means, there can be a local minimum in the free energy with respect to the NCOP and another local minimum corresponding to the COP; a metastable phase separation and a metastable ordering can be simultaneously possible from thermodynamic considerations. The occurrence of one or another will be controlled by the relative

kinetics of both processes; see section 3.1 for full technical details.

In this paper we extend these previous studies by considering the effects of thermal fluctuations (which are shown to have an important effect in the kinetics), and by considering a “double quench” (an initial quench followed by another quench to lower temperature). We chose a specific model, corresponding to a mixture of a liquid crystals and nanoparticles. Liquid crystals are better candidates to display this behavior than solid crystals in real life, because 1 – the higher latent heat of solidification would make it necessary to use very deep undercoolings, and 2 – solidification is comparative slower than liquid crystallization, so the observation of the metastable ordered phase (which is produced by a kinetic effect), might be more difficult. Nevertheless the general physics is in principle valid for any other system that meets the thermodynamic and kinetic conditions required. A one dimensional system will be analyzed in order to study the dynamic, kinetics and generic structural features, avoiding the added computational load of solving the dynamic equations in higher dimension and the complexity of higher-dimensional structures.

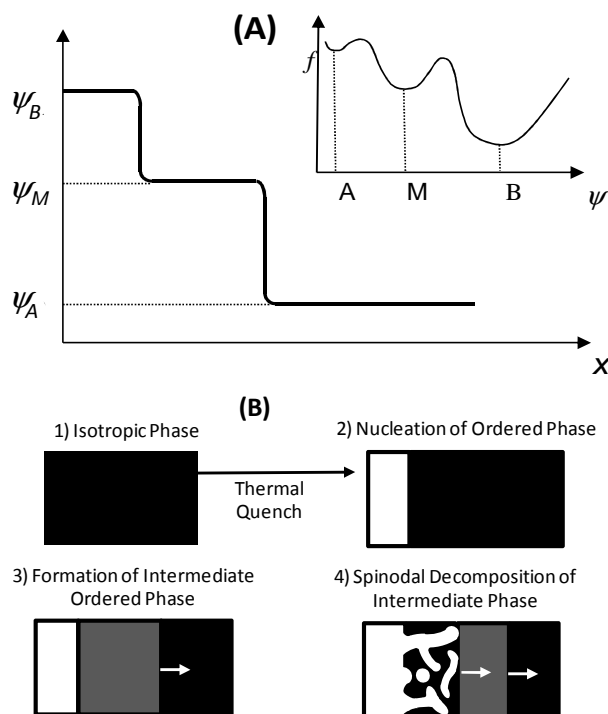


Fig. 1 (A) Schematic illustration of front splitting during a phase transformation for the case of one non-conserved order parameter Ψ . The spatial profiles of the order parameter show two consecutive jumps (split interface), where the metastable phase M is generated between A and B. The inset shows the free energy as a function of Ψ , where a local minimum corresponding to the metastable phase can be seen. (B) Schematic of the process studied in this work: the formation of an intermediate phase which is unstable and decays into the equilibrium phases.

This paper is organized as follows. In section 2 the main equations of the phase-field model used are briefly described. In section 3 simulation results are presented; two types of simulations were performed: (i) single quenches (section 3.1),

and (ii) double quench (section 3.2). Finally, section 4 presents the conclusions.

2. Model

We consider a mixture of non-self-assembling spherical nanoparticles and a nematic liquid crystal. This system is described by two variables: concentration (volume fraction ϕ) and nematic order parameter (S). The Flory-Huggins-Carnahan-Starling theory is used for the mixing free energy, in combination with the Maier-Saupe theory for nematic order. The dimensionless bulk free energy density is:

$$\frac{v_{ref} f_b}{RT} = \frac{\phi_p}{v_{NP}} \ln(\phi_p) + \frac{\phi_{LC}}{v_{LC}} \ln(\phi_{LC}) + \frac{\phi_p}{v_p} \frac{(4\phi_p - 3\phi_p^2)}{(1-\phi_p)^2} + \chi a_p \phi_p \phi_{LC} + \frac{1}{2} \frac{\Gamma}{v_{LC}} \phi_{LC} \phi_{LC} S^2 - \frac{\phi_{LC}}{v_{LC}} \ln(Z) \quad (1)$$

where “P” and “LC” stand for particle and liquid crystal respectively, v and a are volume and surface-to-volume ratio (non-dimensionalized with respect to the reference volume, v_{ref} and $v_{ref}^{2/3}$), ϕ is the area fraction, χ is the mixing interaction parameter, Γ is a Maier-Saupe quadrupolar interaction parameter, R is the gas constant and T is the temperature (non-dimensionalized with respect to the nematic-isotropic transition temperature of the pure liquid crystal). The first two terms are a Flory-Huggins entropy of mixing, the third term is the Carnahan-Starling term accounting for hard-sphere excluded volume effects, the fourth term is a binary interaction (we neglect here anisotropic interactions arising for anchoring effects at the NP surface) and the last two terms are the nematic free energy, where Z is the orientational partition function and it can be well approximated by a polynomial expression in order parameter and concentration. The specific details of the model can be found elsewhere^{17,18}, and will not be analyzed in detail here to avoid lengthy repetitions. Note that the specific form of the free energy would not modify the physics of the process, as long as the thermodynamic conditions (local minimum with respect to NCOP, metastable phase in spinodal conditions), are met.

The free energy density of a non-uniform system is given by¹²⁻¹⁴:

$$f = f_b + f_g \quad (2)$$

where the bulk contribution f_b is given by eq 1, and the gradient contribution, f_g , is given by:

$$f_g = l_\phi \left(\frac{\partial \phi}{\partial x} \right)^2 + l_S \left(\frac{\partial S}{\partial x} \right)^2 + l_{S\phi} \frac{\partial \phi}{\partial x} \frac{\partial S}{\partial x} \quad (3)$$

where l_ϕ , l_S and $l_{S\phi}$ are gradient energy coefficients.

The dynamics of phase transitions can be simulated considering the dynamics of a non-conserved order parameter coupled with a conserved variable (Allen-Cahn-Hilliard equations, also known as model C)¹²⁻¹⁴. The dynamic equations are:

$$\frac{\partial S}{\partial t} = M_S \left(-\frac{\partial f_b}{\partial S} + \frac{\partial}{\partial x} \frac{\partial f_g}{\partial \left(\frac{\partial S}{\partial x} \right)} \right) + \eta_S \quad (4a)$$

$$\frac{\partial \phi}{\partial t} = M_\phi \frac{\partial^2}{\partial x^2} \left(\frac{\partial f_b}{\partial \phi} - \frac{\partial}{\partial x} \frac{\partial f_g}{\partial \left(\frac{\partial \phi}{\partial x} \right)} \right) + \eta_\phi \quad (4b)$$

where M_Q and M_ϕ are the mobilities for ordering and mass diffusion, and η_S and η_ϕ are random thermal fluctuations given by the fluctuation-dissipation theorem (a representative temperature of 300K was used to calculate these terms), and they are implemented as described in ref. [19]. Time and position are expressed in units of the characteristic times and length, $\tau = v_{ref} l_\phi / (M_Q RT_{NI})$ and $l = [v_{ref} l_\phi / (RT_{NI})]^{1/2}$, respectively. Comsol Multiphysics® was used to solve eqs. (4a,4b), by the method of finite elements; standard numerical techniques were used to ensure convergence and stability. The initial conditions are soft step functions in concentration and order parameter, where the concentration of the bulk isotropic phase (ϕ_b) and T are varied, and the initial composition and order parameter in the nematic phase correspond to the equilibrium nematic phase at each temperature, representing a nucleus of equilibrium nematic phase in an undercooled isotropic bulk (except in a particular set of simulations, where the bulk phase is the metastable phase, as will be specified below). The following representative values for the physical parameters were used: $v_c=3$, $v_p=268$, $a_{LC}=4.667$, $a_p=0.75$, $\chi=1.9/T$, $\Gamma=4.54/T$, $l_S/l_\phi=l_{S\phi}/l_\phi=1$. The values of v_c and a_{LC} correspond to a prism of square section and aspect ratio 3, (where the reference volume is a cube with side equal to the smallest side of the prism). As a reference we can consider the liquid crystal 5CB, which has a molecular aspect ratio of approximately 3-3.5. The values of v_p and a_p would correspond to nanospheres with a diameter of 8 nm (which is within the range of typical gold nanoparticles functionalized with short ligands). With the reported values of the physical parameters of 5CB²⁰, $\tau \approx 10^{-6}$ s and $l \approx 1$ nm. Simulations for each initial condition were performed using different values of relative mobility, $M_r = M_\phi / (M_S l^2)$.

3. Results and Discussion

Figure 2 shows the phase diagram used in this work, and the initial conditions of ϕ_b and T used in different simulations are indicated with black circles. Equilibrium phase boundaries are shown as full lines, and the nematic-isotropic transition (NIT) line and the nematic spinodal are shown as dashed lines. The NIT represents the nematic-isotropic transition of a homogeneous phase; below this line a nematic phase has a lower free energy than the isotropic phase, although the state with the lowest free energy within the biphasic region is always a phase-separated state; a homogeneous nematic phase is metastable in this region. The nematic spinodal is the stability limit of a nematic phase, if the concentration of a nematic phase is lower or the temperature is higher than the nematic spinodal, it becomes unstable to concentration fluctuations and undergoes spinodal decomposition²⁰⁻²². Note that the phase diagram is different from the one in ref [14], specifically in this work there is no isotropic-

isotropic phase coexistence. This was adjusted by modifying the value of χ , and the reason of doing so is to avoid further complexity arising from a possible isotropic-isotropic phase separation, so we can isolate the process we aim to study.

Two different kinds of simulations were performed, (i) standard single quenches (cases a-d), where the dynamics and the effect of thermal fluctuations was analyzed, and (ii) a double quench (e), where the simulation was run for a given time isothermally, then a second quench was performed and the simulation was continued using the new temperature. The dashed lines in figure 2 represent the second quench: the horizontal line connects the bulk concentration with the equilibrium concentration of the isotropic phase (concentration at the interface during the first quench). The vertical arrows represents the second temperature quench, so the tip or the arrow indicates the position of the bulk and the interface after the quench.

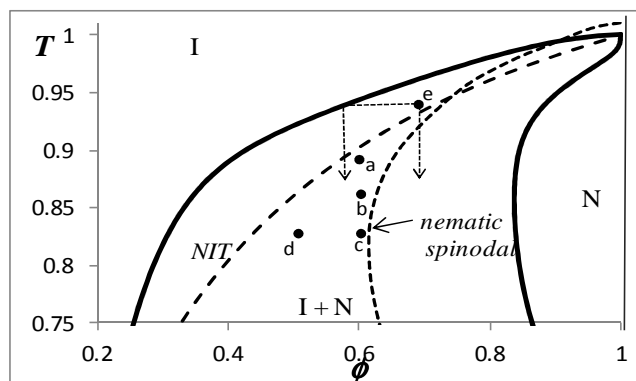


Fig. 2 Computed phase diagram based on eqn. 1; for: $v_c=3$, $v_p=268$, $a_{LC}=4.667$, $a_p=0.75$, $\chi=1.9/T$, $T=4.61/T$. I and N represent the stable phases, I + N indicates phase coexistence. Full lines indicate equilibrium binodal lines, dashed lines indicate the NIT line and the nematic spinodal. The positions a, b, c, d and e indicate the initial conditions used in the simulations.

3.1 Single quenches (cases a-d)

In all these cases, the initial conditions are comprised between the NIT line and the nematic spinodal. In this region, a nematic phase is metastable, in the sense that it is more stable than the isotropic phase, but it is unstable with respect to concentration fluctuations, so the conditions for the formation of an oscillating front, characteristic of spinodal decomposition, are met. The main goal of this section is to analyze how the evolution of this fluctuating front is affected by thermodynamic (position in the equilibrium phase diagram (Fig.2)) and kinetic (relative mobility M_r) factors, and specially how thermal fluctuations affect this evolution.

The intermediate homogeneous nematic phase is formed by a kinetic front-splitting mechanism, as described in previous works¹²⁻¹⁴: when the relative mobility M_r is small enough, the original interface spontaneously splits in two and the metastable phase appears between the equilibrium nematic phase and the undercooled bulk isotropic phase. This process is very similar to that described in refs. [8-13] (the difference is that in refs. [8,9] no conserved variable was involved, and in ref. [12,13] the intermediate phase was isotropic). If the relative mobility $M_r = M_\phi/(M_S l^2)$ is larger, no front-splitting is observed and the system evolves as a regular diffusional phase transition described by

Ficks`s diffusion law. The critical value of relative mobility required for front splitting, $M_{r,c}$, is a function of the position in the phase diagram: it decreases as the NIT line is approached, and obviously at and above the NIT line front splitting does not take place so $M_{r,c} = 0$. It was found that $M_{r,c}$ follows a linear functionality with $\phi - \phi_{NIT}$, where ϕ_{NIT} is the concentration of the NIT line at the simulation temperature. This is shown in figure 3.

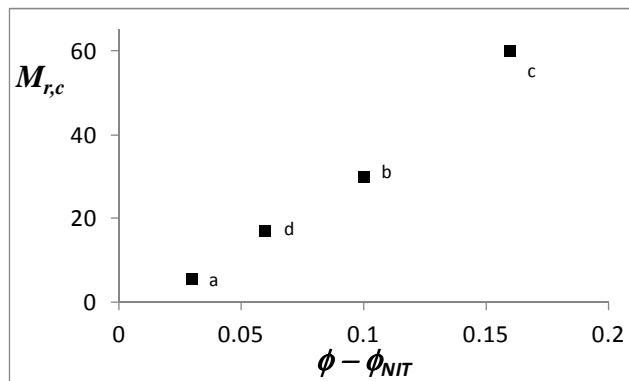


Fig 3 Critical value of relative mobility for the formation of the split-front, as a function of $\phi - \phi_{NIT}$. Cases a-d are indicated.

As described above, the intermediate nematic phase is unstable to concentration fluctuations. The existence of a sharp interface itself, (which can be viewed as a large, localized, stepwise fluctuation) is enough to trigger spinodal decomposition even in the absence of random thermal fluctuations. This spinodal decomposition is initiated at the interface, and propagates towards the bulk producing the oscillating front right after the metastable phase is formed, as shown in figure 4. The velocity of the oscillating front produced by this mechanism is relatively small, and independent of the velocity of the leading N-I front as described in refs. 15,16. In addition, in the presence of thermal fluctuations, regular bulk spinodal decomposition will take place. But as the nematic phase is formed through a moving front, the bulk spinodal will also evolve as a moving front, with the same velocity as the leading front. In addition, it takes some time until the fluctuations (initially very small in amplitude) grow to a significant value and the oscillating structure becomes noticeable. Consequently, it can be considered that there is a "latency period" until the bulk spinodal becomes noticeable (this latency period depends on the amplitude of thermal fluctuations), after which the oscillating front moves at the same velocity as the leading front. So two different mechanisms for the formation of the oscillating front can be identified: an interface-induced spinodal and a moving bulk spinodal.

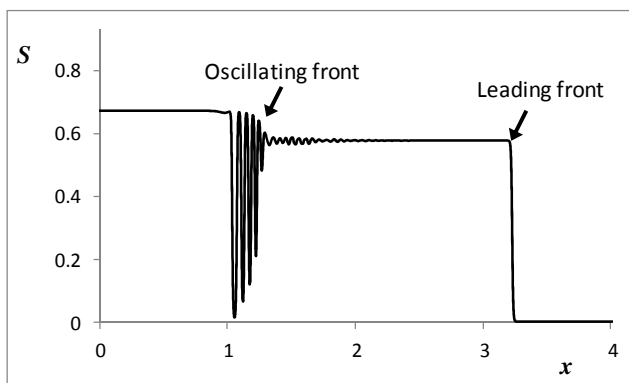


Fig. 4 Order parameter profiles for case "a" as a function of dimensionless position and $M_r=5$, at dimensionless time $t=20000$, showing the intermediate phase and the oscillating front.

Figures 5 (a) and (b) show the velocities of the oscillating front produced by the interfacial-induced spinodal and by the moving bulk spinodal (which is equal to the velocity of the leading front), respectively. These velocities were calculated by tracking the position of the oscillating front, which was defined as the point where the envelope of the oscillating structure has an inflection point. In order to observe the interfacial-induced spinodal without interference of the second mechanism, simulations without thermal fluctuations were performed, and using the metastable nematic phase as bulk phase in the initial conditions (this reduces pseudo-fluctuations produced by numerical error, that can also trigger bulk spinodal decomposition).

The velocity of the interface-induced oscillating front is directly proportional to the mobility and an increasing function of $\phi - \phi_{\text{SPIN}}$, where ϕ_{SPIN} is the concentration of the nematic spinodal, while the velocity of the moving bulk spinodal front is a linear decreasing function of the relative mobility, and a monotonic decreasing function of $\phi - \phi_{\text{NIT}}$. As can be seen, the velocity of the front produced by the first mechanism has the same variable dependences as the regular bulk spinodal, while the second mechanism, which is a true bulk spinodal, has a different behaviour. This can be understood considering that, as described before, the velocity of the moving bulk spinodal front is actually controlled by the leading front, which is a regular interface separating two bulk phases. The velocity of this front is controlled by the degree of undercooling or supersaturation, hence the dependence on $\phi - \phi_{\text{NIT}}$ and not on ϕ_{SPIN} .

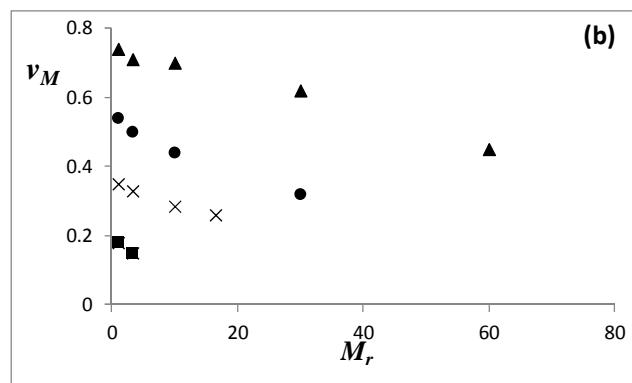
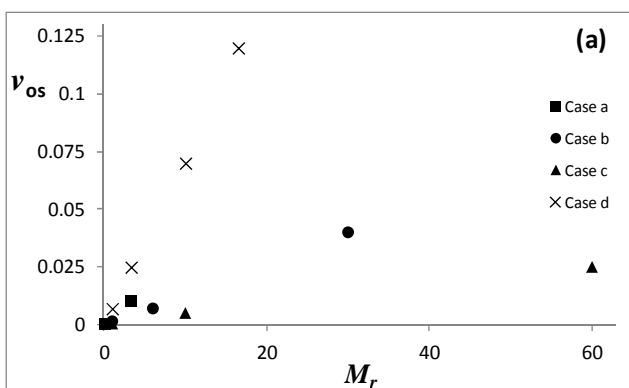


Fig. 5 (a) Velocity of the oscillating front produced by the interface-induced spinodal decomposition. (b) Velocity of the leading front, which is equal to the velocity of the oscillating front produced by the moving bulk spinodal.

The explanation of why the velocity decreases when the relative mobility increases is less obvious, but can be understood as follows. This front is an interface separating an ordered phase and an isotropic phase, both with the same composition. As no mass diffusion seem to be involved, this process should in principle not be affected by the relative mobility (recall that the characteristic time is defined in terms of the ordering mobility, so the relative mobility is significant only in the presence of diffusion). But actually, at the interface, a small peak in concentration is formed (due to the coupling term in the gradient free energy), so there is a small coupling between ordering and diffusion. As the diffusivity increases, the influence of diffusion, although it remains small, increases, thus having a stronger effect on the dynamics of this front. As diffusion is the slow process, this stronger coupling implies a slower front. Recall that when the relative mobility is large enough ($M_r > M_{r,c}$), front splitting does not take place and the whole process is controlled by diffusion (and it is much slower).

Considering the two mechanisms described, at very short times, the oscillating front is produced by an interface-induced spinodal decomposition mechanism, and it moves very slowly, but after some time (latency period), the moving bulk spinodal mechanism is observed and the oscillating front moves at the same velocity as the leading front. Note that there is a single oscillating front, but two different kinetic regimes corresponding to each mechanism. This is shown in Fig. 6, where the position of the oscillating front for case d and $M_r = 3.3$ is plotted as a function of time. The two limiting cases of interface induced oscillating front, $x = v_{os}t$ at short times, and the moving bulk spinodal front $x = v_M(t - t_{\text{lat}})$ at long times are also plotted (t_{lat} is the latency time, chosen as $t_{\text{lat}} = 9100$ to fit the observed velocity). As a consequence of this (the oscillating front moving at the same velocity as the leading front after some time), the metastable region reaches a maximum size and then it remains constant, unlike the cases studied in ref [14] (where it grows unbounded), and refs [12,13] (where it grows and shrinks, displaying a finite lifetime). The position of the leading front is also plotted in figure 6 to illustrate this fact.

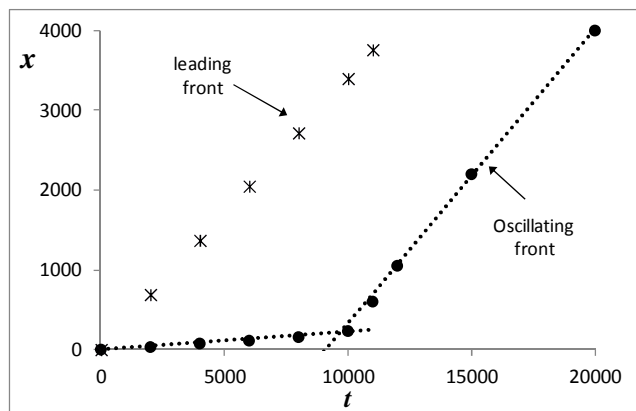
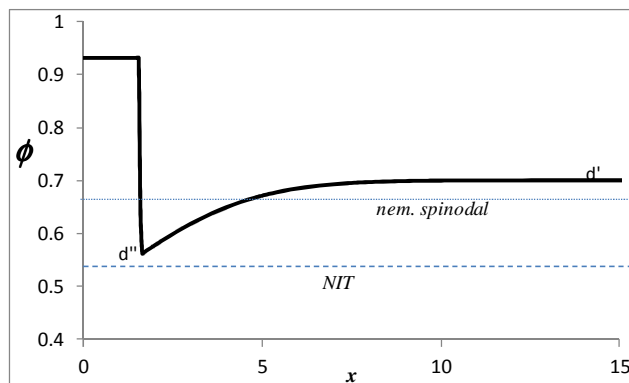


Fig. 6 Position x of the two different fronts as a function of time. The dotted lines represent the interface-induced spinodal front (smaller slope), and moving spinodal front (larger slope). See text.

5 In this paper we limited the study to the one-dimensional case, in higher dimensions there is a variety of structures that can be formed. Some two dimensional simulations results can be found in ref [15], where three main structures were observed: concentric rings, dispersed droplets and radial branching. Any of these
 10 structures can be expected as the higher dimensional form of the oscillating front (depending on the physical parameters), but the generic dynamic and kinetic features observed in one dimension should be the same in higher dimensions.

3.2 Double thermal quench (case e)

15 In case e, a double thermal quench was simulated, where a first quench is performed into the biphasic region of the phase diagram, but above the NIT line (no front splitting), and after some time, a second quench below the NIT line is performed. This double quench could be a better representation of real
 20 experiments, where cooling is not instantaneous and the system will spend a finite time in each region of the phase diagram crossed by the cooling trajectory (so it would give qualitatively the same results).



25 **Fig. 7** Concentration profile for the first quench at $t = 10^8$, right before the second quench is applied. The concentrations corresponding to nematic spinodal and NIT line for the temperature of the second quench are also shown.

As we are dealing with the case of small relative mobility, in
 30 the first quench the process is kinetically controlled by diffusion, so the concentration in the isotropic phase at the N-I interface will be given by the equilibrium concentration, and concentration profiles as described by Fick's law are produced. This is shown in figure 7, which is a snapshot of this process at $t = 10^8$, right
 35 before the second quench is introduced. The second quench is performed such that the bulk phase is in the stable nematic region of the phase region, while the interface lies between the NIT and the nematic spinodal. This is indicated by the arrows in figure 1, and also the NIT and spinodal concentrations after the quench are
 40 shown in fig. 7.

As now the whole isotropic phase is below the NIT line, a metastable nematic phase can be produced by an interface-splitting mechanism as before. Close to the interface, this phase is in spinodal conditions so an oscillating front should be produced, but in the bulk, the nematic phase is the stable region of the phase diagram, so the spinodal front cannot propagate into this zone. As a consequence, the oscillating front is produced and moves until it reaches a position where the concentration is close to ϕ_{SPIN} , and then it stops, so that the oscillating structure is confined in a
 45 region close to the interface ("mushy region"). This is shown in figure 8, where figs 8(a)-(c) show concentration and order parameter profiles for different times, and fig 8(d) shows the position of the oscillating front as a function of time. Note again that there is an increase of velocity at an approximate time of
 50 80000 (corresponding to the transition from interfacial-induced spinodal to moving bulk spinodal), and then the front slows down. Once the mushy region is fully developed, further evolution proceeds through a diffusive mechanism as will be explained below.

Cite this: DOI: 10.1039/c0xx00000x

www.rsc.org/xxxxxx

ARTICLE TYPE

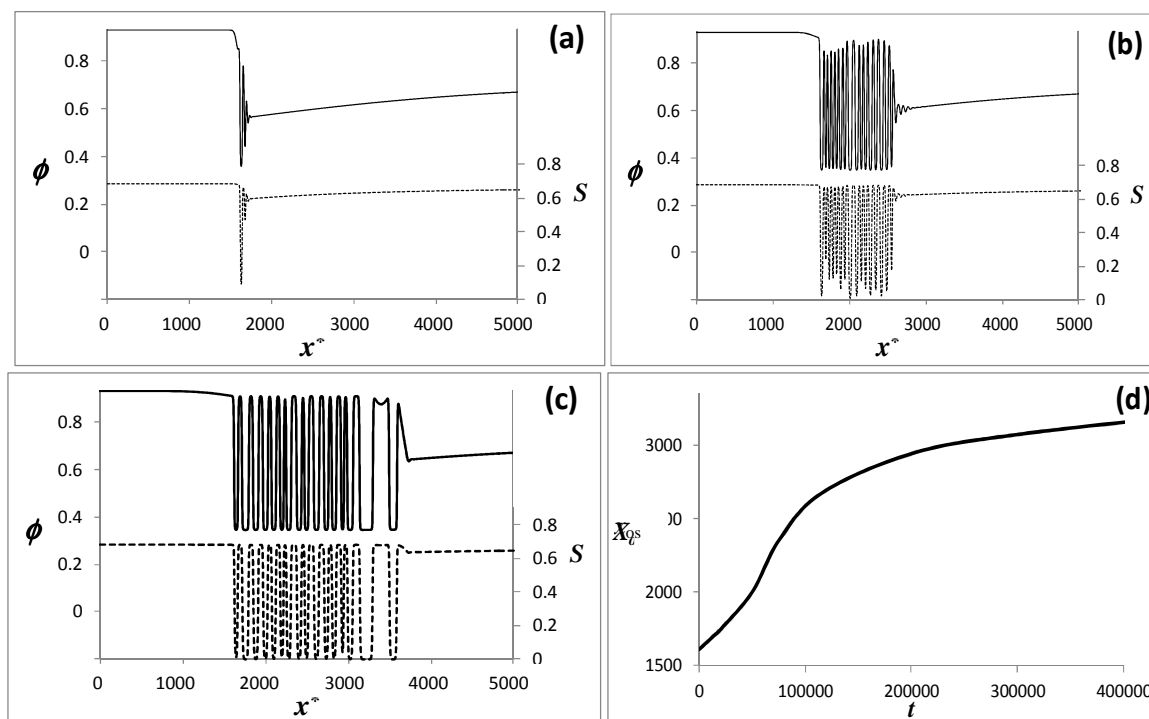


Fig. 8 (a) – (c) Concentration (solid, left axis) and order parameter (dashed, right axis) profiles after the second quench, for $t = 12000$ (a), $1.1 \cdot 10^5$ (b), and $1.4 \cdot 10^6$ (c). (d) Position of the oscillating front as a function of time.

5 The long-time evolution of the system leads to a very different phase morphology from that of a typical phase growth process, and it is shown in figure 9. While the mushy region remains and coarsens with time, the last composition “valley” grows, producing the isotropic phase, and the concentration in the bulk
 10 slowly increases to the equilibrium value through a Fickian diffusional process. The bulk, originally isotropic, is turned into the nematic phase (without further nucleation of more nematic domains) while the isotropic phase is formed and grows in a region close to the original nematic nucleus. Now the isotropic phase grows into the nematic bulk, as opposed to the original
 15 situation where the nematic phase was growing into an isotropic bulk.

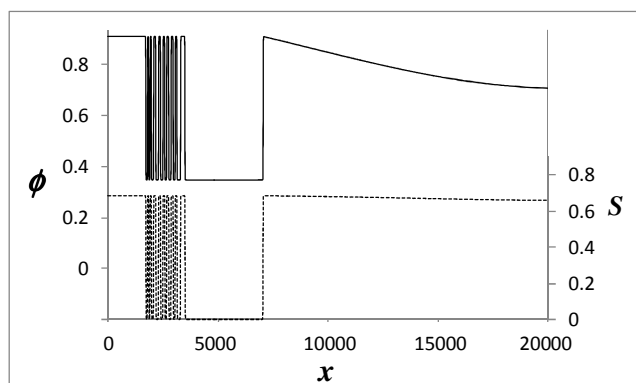


Fig. 9 Concentration (solid, left axis) and order parameter (dashed, right axis) profiles at very long time ($t=10^9$) after the second quench.

Conclusions

Phase transformation of a mixture of liquid crystals and nanoparticles, a thermodynamic system described by coupled COP and NCOP, was studied under conditions where an
 20 oscillating front can be formed by a front-splitting instability followed by spinodal decomposition, by means of a phase-field model based on the direct integration of the well-established Maier-Saupe and Flory-Huggins equations (Eqs.(1-4)). The evolution of the oscillating front and the effect of thermal
 25 fluctuations for different thermodynamic and kinetic conditions were studied. Two mechanisms for the formation of an oscillating front were observed to coexist: an interface-induced spinodal, where the oscillating structure is generated at the interface and propagates into the bulk, and a moving bulk spinodal, which is a
 30 regular bulk spinodal initiated by thermal fluctuations in a bulk phase that is produced through a moving front. At short times the first mechanism prevails and the front moves with a small velocity, while at longer times the second one dominates and the oscillating front moves at the same velocity as the leading front
 35 (Fig.6). This results in the metastable phase being confined to moving region of constant finite size, as opposed to other cases of double front formation analyzed in the literature mentioned above.
 40

The effect of performing a double quench was also analyzed, in the spirit of better representing a cooling experiment in real life where the material system will spend a finite time in each region of the phase diagram. For adequate conditions (this is, after the second quench bulk composition has to be higher than ϕ_{NIT} and the concentration at the interface, bounded between ϕ_{NIT} and ϕ_{SPIN}), the oscillating front forms but it remains confined to a region close to the interface, while the bulk, originally isotropic, becomes nematic, and the equilibrium isotropic phase is formed close to the initial nematic nucleus and grows towards the bulk nematic phase (Figs.8,9). This is the opposite of the initial (and typical) growth where the nematic nucleus grows into the isotropic bulk (Fig.4).

In summary, the present work demonstrate significant new structural and dynamical features in phase transformations in mixtures of mesogens and non-mesogen components, arising from generic thermodynamic and transport features in multiple order parameter systems. In particular spinodal decomposition in intermediate phases is a novel phenomenon to structure mesogenic materials using simple quenching methods.

Acknowledgements

The National Research Council of Argentina supported E.R. Soule. This study is based on the research done by A.D. Rey supported by the U.S. Office of Basic Energy Sciences, Department of Energy, grant DE-SC0001412.

Notes and references

1. A. Onuki, *Phase transition dynamics* Cambridge, UK, Cambridge Univ Pr; 2002.
2. S. Z. D. Cheng *Phase transitions in polymers: the role of metastable states*, Elsevier Science; 2008.
3. E. Foard, A. Wagner, *Physical Review E*. 2012, **85**, 011501.
4. P. Hantz, I. Biro, *Physical review letters*. 2006, **96**, 088305.
5. W. Shi, H. Cheng, F. Chen, Y. Liang, X. Xie, C. C. Han., *Macromolecular Rapid Communications*, 2011, **32**, 1886.
6. H. Tanaka, T. Nishi, *Physical Review A*. 1989, **39**, 783.
7. H. Tanaka, T. Nishi, *Physical review letters*. 1985, **55**, 1102.
8. J. Bechhoefer, H. Lowen, L. S. Tuckerman, *Physical review letters*, 1991, **67**, 1266.
9. L. S. Tuckerman, J. Bechhoefer, *Physica A: Statistical Mechanics and its Applications*, 1992, **46**, 3178.
10. N. M. Abukhdeir, A. D. Rey, *Macromolecules*, 2009, **42**, 3841.
11. L. M. R. Evans, K. W. C. Poon, *Physical Review E*, 1997, **56**, 5748.
12. E. R. Soule, A. D. Rey, *European Physics Journal B*, 2011, **83**, 357.
13. E. R. Soule, A. D. Rey, *EPL*. 2009, **86**, 46006.
14. E. R. Soule, C. Lavigne, L. Reven, A. D. Rey. *Physical Review E*, 2012, **86**, 011605.
15. M. Zukerman, R. Kupferman, O. Shochet, E. Ben-Jacob, *Physica D: Nonlinear Phenomena*, 1996, **90**, 293.
16. K. Glasner, R. Almgren, *Physica D: Nonlinear Phenomena*. 2000, **146**, 328.
17. E. R. Soule, L. Reven, A. D. Rey, *Molecular Crystals and Liquid Crystals*, 2012, **553**, 118.
18. J. Milette, V. Toader, E. R. Soule, R. B. Lennox, A. D. Rey, L. Reven, *Langmuir*, 2013, **29**, 1258.
19. R. Petschek, H. Metiu, *The Journal of chemical physics*, 1983, **79**, 3443.
20. J. R. Dorgan, *Fluid Phase Equilibria*, 1995, **109**, 157.
21. C. C. Riccardi, J. Borrajo, R. J. J. Williams, *The Journal of Chemical Physics*, 1998, **108**, 2571.
22. E. R. Soule, A. D. Rey, *Molecular simulations*, 2012, **38**, 735.